Simulation of ETAS Earthquake Catalog Using Artificial Intelligence (AI)

James Zhang*

University of California, Davis, CA, USA

E-mail: txjzhang@ucdavis.edu

Abstract

The Epidemic Type Aftershock Sequence (ETAS) model was proposed to quantify the earthquake event and its following aftershock events by Ogata in 1988.[1] In this paper, we construct this ETAS model in a different way by improving the python codes generated from Large Language Model chatGPT from openai.com. This program generated by Artificial Intelligence (AI) follows the basic feature of the model including Omori law of aftershock decay, Gutenberg-Richter law expressing relationship between Earthquake numbers and magnitude, and Bath law identifying the aftershocks. Surprisingly, an AI-generated python code also includes a scale invariant re-clustering feature that arranges the aftershock magnitude with respect to the frequency influenced by the geometric feature of Omori decay's law. Further, historical data in California from 1970 to present are applied on a real map to help quantitatively measure the deviation with simulated results. In the future, this programme can be engaged with a transformer model in deep learning,[2] and thus provide with an accurate prediction of future earthquakes.

Introduction

Aftershocks are series of earthquakes that happen right after the major earthquake, which is called mainshock, and they often happen more frequently with less magnitude. Some aftershocks may last between a week to several months.[3] Although aftershocks have a less magnitude, they still come with a destructive power, which could repeatedly cause serious damages to the buildings and landscapes. Let's take Wenchuan Earthquake as an example. The 2008 Wenchuan Earthquake happened in Sichuan Province, China was the largest earthquake with huge amount of landslides within past 100 years.[4] The main earthquake reached a magnitude of 7.9 while numerous of aftershocks were observed.[3,5] The mainshock only lasted for 2 minutes and it didn't bring gigantic damages compared with those aftershocks.[4] But for aftershocks that are larger than magnitude of 5, they lasted for 745 days, while various small aftershocks were not recorded.[3] Since this earthquake affected a large area within Sichuan Basin, which had diverse landscapes and dense populations, disastrous damages were caused by these aftershocks, including landslides, quake lakes, mudflows, building collapses and breakdown of supply.[5] And these damages, along with the earthquake itself, resulted in more than 90,000 people death or missing.[4,5] Therefore, not only the mainshock but also aftershocks can result in severe damage and researchers are finding a method to model these aftershocks and try to predict it in the near future.

Since aftershocks are always induced by previous earthquake shocks, it can be either mainshock or aftershock, there are different types of aftershocks during the whole earthquake event. The first type is called primary aftershocks which are directly triggered by the mainshock, while secondary aftershocks is a second type aftershocks that are triggered by the primary aftershocks.[6] Therefore, an earthquake event, either mainshock or aftershock, always increase the probability of aftershocks at a later time. In this manner, a mainshock always triggers several primary aftershocks, and these aftershocks also trigger more sec-

ondary aftershocks, and mixed types of aftershocks often appear at the same time so that it looks like the spread of a epidemic disease.

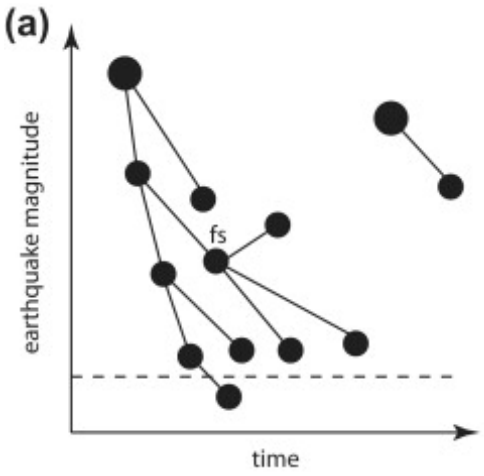

Figure 1: Schematic Diagram for earthquake branching.Large circles represent spontaneous events. Dashed line indicates ground motion. fs: a small mainshock succeeded by the earthquake of larger magnitude.[7] Reproduced from Geist (2012)

Since all the aftershocks depend on each other as shown in figure 1, we can model this chain to be a branching process model. Therefore, a background rate, μ, will be set in this model to account for the constant loading rate that is due to the tectonic plates motion.[7] So in this branching process model, we will have a background rate and aftershocks' rate that are due to the triggering of previous earthquakes. In 1988, Epidemic Type Aftershock Sequence (ETAS) model was proposed by Yosihiko Ogata taking advantage of aftershocks' widespread characteristics. It incorporated with various statistical methods.[1] This model focuses on aftershock activities influenced by the occurrence of a main earthquake and finds several characteristics of the overall aftershocks, including the frequency, magnitude, and duration. Moreover, three statistical laws are discovered that fit this model.[1]

Based on these laws, ETAS model can be written mathematically to find the intensity of each aftershock.[1]

$$\lambda(t,x,y) = \mu + \sum_{i:t_i^c<t} g(t-t_i^c)e^{\beta(M_i^c-M_r)}f(x-x_i,y-y_i) \tag{1}$$

Here μ is the background seismicity rate, g and p are parameters for frequency decay, t_i^c is the primary event time, M_r is the minimum magnitude threshold, β is the parameter to scale number of events with event magnitude M_i^c, and f(x,y) is the spatial distribution.[1] Below are the three laws from the ETAS model and explanation of each

parameters.

Gutenberg-Richter law

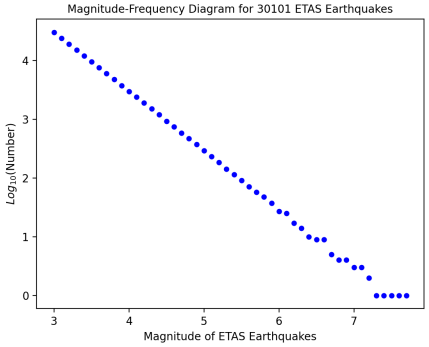

Figure 2: Example of Frequency and Magnitude relationship with 30101 earthquakes observed in Gutenberg-Richter Law. Magnitude of aftershocks are bounded between 3 to 8

Gutenberg-Ritcher Law describes the relationship between the magnitude and frequency of the earthquake occurrence, and they model this with a simple equation[8]

$$\log_{10} N = a - bM \tag{2}$$

where M is the magnitude of the aftershocks, N is the number of magnitude larger than the magnitude M which is also known as the frequency, a and b are both constants. As shown in Figure 2, this equation describes a decrease of frequency as the magnitude M increases, which makes sense intuitively as aftershocks with smaller magnitude will happen more often. Since Gutenberg-Richter law describes the aftershocks and their frequency generally here, there is no need to distinguish between the primary aftershock and secondary aftershock. Other researchers also discover that b value in this law should be between 0.5–1, with some exception case that is larger than 1.[9,10]

Omori-Utsu Law

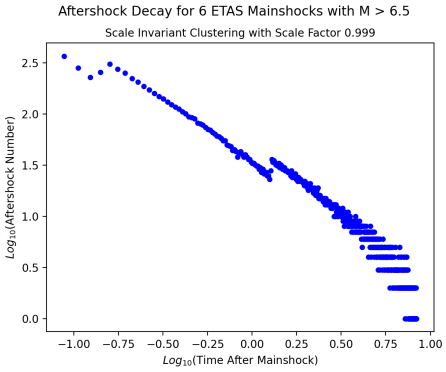

Figure 3: Example of Omori-Utsu Law of aftershocks decay between 0–10 days

Omori-Utsu Law describes the frequency decay of aftershocks over time after the strong mainshock.[11] This law describes

the frequency decay with an equation[1,11,12]

$$N(t) = \frac{k}{(c+t)^p} \tag{3}$$

Here t is the time since the occurrence of the mainshock, N, again, is the number of aftershocks at time t, and K, c, p are all parameters. As shown in 3, the frequency of aftershocks decreases as time increases, and this fits the limiting behavior that the aftershocks will die off at infinite large time. For these parameters, K depends on the lower bound of the aftershocks that is being counted[1] and p is usually 0.9 – 1.5.[12] Using this law, Utsu himself even discovered that the aftershocks of Nobi earthquake in 1891 last for at least 80 years.[1]

Bath's Law

Bath's Law claims that the difference between the magnitude of mainshock and the magnitude of largest aftershock is a fixed number,[13] and we show this difference as ΔM.

$$\Delta M = 1.2 \tag{4}$$

This law is surprising because it shows that the largest magnitude of aftershocks is actually independent of other aftershocks, and it's only dependent on the magnitude of mainshock. Based on aftershocks classification, the secondary aftershocks are only triggered by the primary aftershocks, so it is obvious that the largest aftershocks should be the primary aftershocks that only depend on its mainshock.

Improvements of the Model

We realize that this model includes lots of parameters, and the tuning and exploration of these parameters is also a big problem for simulation. In order to improve the model for better prediction, different types of improvement have been proposed. Due to the limit of computation, researchers focused on the method to minimize the cost when conducting ETAS simulations. Several studies introduced an approximation using a maximum likelihood method to simplify the integral calculation, which not only speeds up the computation time, but also provides the sta-

ble results.[14,15] Moreover, they discovered the poor performance of this model when the size of the earthquake catalog is small, which is because less data results in less correlation of parameters in the model.[15] Other studies discussed the bias of parameters due to the various deficiencies of earthquake data, such as insufficient data during short term incompleteness of magnitude, which is created by the blinding of detecting algorithms. In order to remove this, they proposed a new variable blinding time T_b to account this deficiency and found higher maximum-likelihood values.[16] For value p in Omori-Utsu law specifically, researchers also found its limit on the aftershocks estimation due to the assumption of infinite triggering time[17] This limit is made due to the assumption of a stable solution of the ETAS model. However, observed data show that assumption of static stress change may not be true, which makes the range of p value to be larger, and current choice of p value is thus biased. To make p value unbiased, finite triggering time was proposed by introducing a new parameter T_a, finite duration time, and this modified model helped to determine the effective forecasting period of original ETAS model.[17]

Another aspect of improvement is to apply this model in some other areas other than focusing on epidemic type aftershocks. For example, Helmstetter et al. applied ETAS model to provide a daily earthquake probability, and they found this model had a better performance when forecasted aftershocks with smaller magnitude in short term,[18] and other study applied this model to detect the geothermal events such as magma intrusion.[19]

With these discussions of the potential improvements of the model, we now have a basic idea of how parameters should behave in our model, so we can use it to compute rates of expected activity, based on an assumed background seismicity rate using California earthquake data. With the sophistication of artificial intelligence, coding can be done with the computer's help. In this paper, we developed an ETAS model using Python based on the code generated by the Large Language Model chatGPT from openai.com. Surprisingly, this

AI based program works well and three statistical laws are still present with features that can cluster the aftershocks based on criteria on time scale. For example, it filters the aftershocks that are loosely connected to the mainshock or primary aftershock based on time. Furthermore, this program was improved to be a catalog that could potentially predict earthquakes around the world. Here we include the physical locations of Los Angeles area from $37°N$ and $122°W$ to $29°N$ and $113°W$ to run the aftershock simulations and compare it with the historical LA earthquake data in the same area.

Computational Details

The ETAS simulation program was written in Python based on the code provided by Large Language Model ChatGPT from openai.com. ChatGPT was asked to provide a Python code about the ETAS model first with a series of random generating functions to provide background events, aftershock events, as well as the events with random locations. With the input of initial parameters, this script could generate a figure showing synthetic aftershocks with randomly generated locations.

After testing this ChatGPT generated code, figures of GR plot and Omori decay were plotted to examine the behavior of three statistical laws behind the ETAS model. We then improved this script to include real earthquake data downloaded from the United States Geological Service (USGS) `https://earthquake.usgs.gov/fdsnws/event/1/`. What's more, the simulated aftershocks from 1969 till now were produced based on geological information of Los Angeles downloaded from USGS. For the simulated aftershocks, parameters were preset and simulations started in the given area. After one simulation was done, it repeated until the parameters were optimized to find the most accurate result. Lastly, we developed another Python code to analyze and quantify the difference between the simulated earthquakes and real data.

Results and Discussions

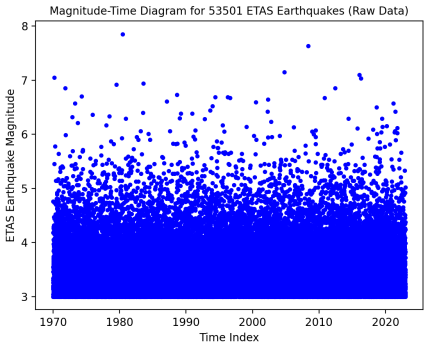

Figure 4: Unclustered simulated aftershocks generated from 1970 to 2023

Interestingly, this ChatGPT generated code includes a new feature to recluster the magnitude of aftershocks with respect to time shown in Figure 4 and Figure 5. In Figure 4, we find a messy picture that shows 53501 generated aftershocks with their magnitudes and time. However, some aftershocks are triggered by other lower level aftershocks, such as tertiary aftershocks or even less. Moreover, some other aftershocks that have a high magnitude are also filtered out due to its long elapsed time from the mainshock which is inconsistent with the Omori-Utsu Law.[11] These aftershocks are not in our consideration so the AI created code includes the cluster feature to filter out the useless aftershocks. Figure 5 shows the clustered aftershocks with their magnitude and time.

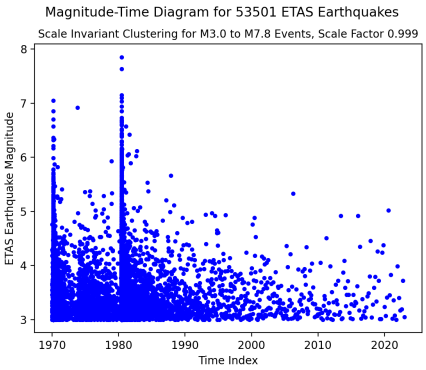

Figure 5: Clustered simulated aftershocks generated from 1970 to 2023

Compared with Figure 4, we find only two obvious peaks left. The two peaks (around 1970 and 1981) are the largest aftershocks following the mainshocks, and they are both larger than magnitude of 7. Aftershocks also happen rapidly that year with a huge amount of aftershocks in the following years, which fits the frequency trend of GR law[8] and exponential decay of Omori-Utsu law.[11] Around 2008, there is an aftershock at magnitude around 5.5, which shows the sign of primary aftershocks due to a mainshock around the same time. It can be seen that there is an increasing amount of aftershocks at a smaller magnitude soon after that, but it doesn't

show an obvious pattern as two left peaks. The recluster that filters out the aftershocks may cause the lack of peak pattern here. With this recluster feature, it is much easier to find the trend of earthquakes with a high peak and bunch of aftershocks, but it may not be accurate for long term.

Now we show the relationship between magnitudes and frequency of the simulated aftershocks to check this AI generated ETAS model.

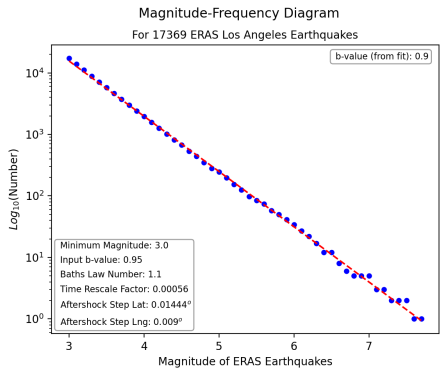

Figure 6: Magnitude and Frequency Plot of ETAS Model. Blue dots are the simulated aftershocks, and the red dashes are the best fit line. Threshold of aftershock magnitude was is set to be 3.0.

Shown in Figure 6, red dashed lines are the best fit linear line of the magnitude-frequency diagram, and this pattern shows the Gutenburg-Richter law,[8] with a optimized b value at 0.9. We find that this law fits pretty well with magnitude smaller than 6. For larger magnitudes, this line doesn't follow the simulated results, which is also mentioned in previous study.[17] However, we think this is trivial because it is rare to have aftershocks with such large magnitudes, and we don't have enough simulated data to show this relation.

Moreover, figure 6 also reports the magnitude difference between the mainshock and largest aftershock as Baths Law Number, and we got it to be 1.1 ± 0.1, which is close enough to the Bath's law number of 1.2. Next, we report the magnitude change with respect to time.

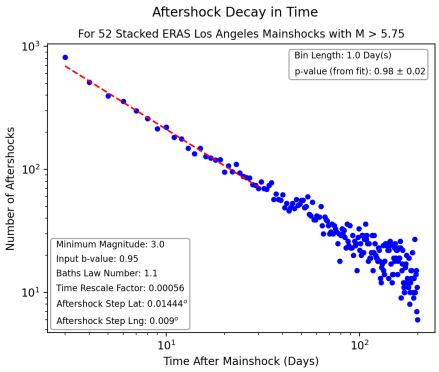

Figure 7: Plot of clustered aftershock of ETAS Model within 125 days. Blue dots are the number of simulated aftershocks within 1 day, and the red dashes are the best fit line. Threshold of aftershock magnitude was is set to be 3.0.

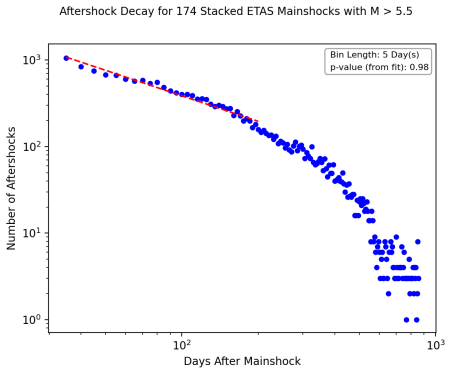

Figure 8: Plot of clustered aftershock of ETAS Model within 1000 days. Blue dots are the number of simulated aftershocks within 5 day, and the red dashes are the best fit line. Threshold of aftershock magnitude was is set to be 3.0.

Figure 7 shows the pattern of Omori-Utsu law, which presents the decay of aftershocks with longer time. And we created a fitted line from 0 days to 15 days to show this law. It turns out the fitted line runs pretty well at an early time (before 125 days). However, as shown in Figure 8, this Omori decay decreases more rapidly after 4 months, and eventually dies off around 2.5 years. For both figures, we find the optimized p-value is 0.98 ± 0.02. For our simulations, we use the optimized parameters of the original ETAS model[1] so that it can always result in more accurate results

Finding these three laws from the AI based ETAS Model, we try to simulate aftershocks with real geological information downloaded from USGS. Here we report the aftershocks in Los Angeles. Figure 9 and figure 10 respectively show the real earthquake data and simulated earthquake data of the Los Angeles area from 1969 to 2024. Since earthquakes contain both mainshocks and aftershocks, it is hard to directly distinguish them on the map. However, the number of aftershocks is far larger than that of mainshock for such a long period, so generally we ignore this difference during the quantitative comparison.

Comparing Figure 9 and Figure 10, we notice a few differences between the real data and simulated one. For example, there was an earthquake with $M \geq 6.9$ around $37°N$ and $122°W$, but simulated data only shows a smaller magnitude earthquake. However, there are still similar trends between the simulated data and real earthquakes, such as three strong earthquakes with $M \geq 6.9$ as well as a group of smaller earthquakes with $M \leq 5.9$. Therefore, we can still use these simulated earthquakes for future prediction.

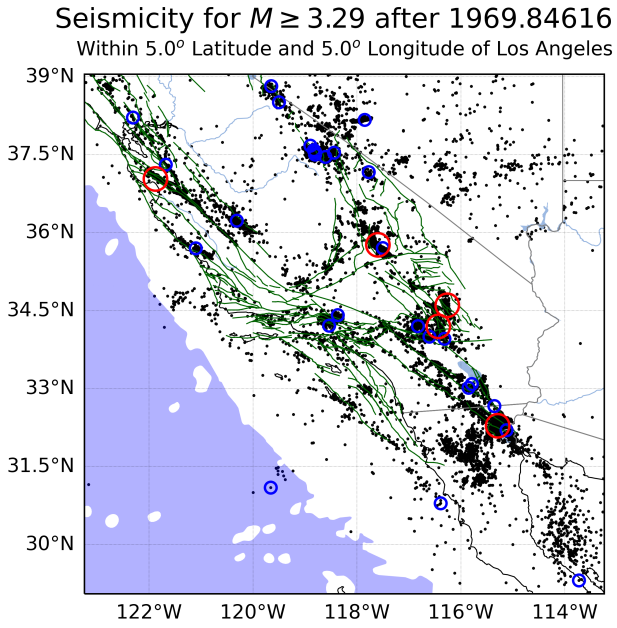

Figure 9: Historical earthquakes map around Los Angeles area from November 1969 to January 2024. Area with red circle shows magnitude larger than 6.9. Blue circle area shows magnitude between 6.0 to 6.9. Black dots are aftershocks between 3.29 to 5.9.

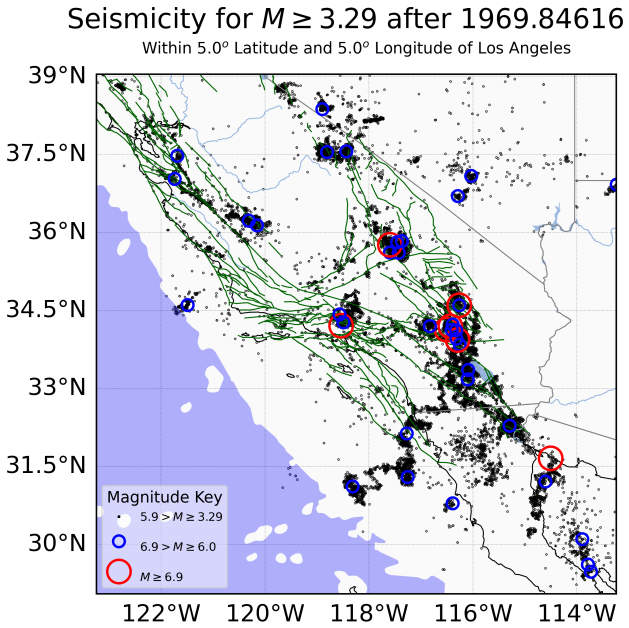

Figure 10: Simulated earthquakes map around Los Angeles area from November 1969 to January 2024. Area with red circle shows magnitude larger than 6.9. Blue circle area shows magnitude between 6.0 to 6.9. Black dots are aftershocks between 3.29 to 5.9.

Lastly, in order to quantify the difference between real data and simulated earthquakes over time, we define this difference as a spatial magnitude deviation ΔM_s.

$$\Delta M_s = \Sigma (M_{sim} - M_{real})^2 \qquad (5)$$

In order to calculate ΔM_s, we find the location of simulated earthquakes that match real data. Then, we directly take the difference between these two values and square it to find all values positive. Therefore, in the limiting behavior, a perfect simulated data should result in 0. And the less ΔM_s is, the more accurate our simulation is. Obtaining 25 simulations, we find average deviation is 0.40 ± 0.08.

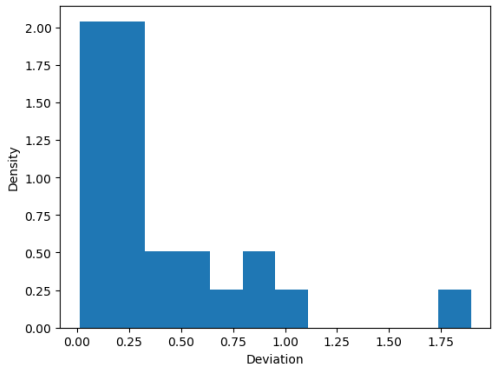

Figure 11: Probability density of the spatial magnitude deviation under 25 simulations.

Figure 11 shows the histogram of ΔM_s from 25 simulations. It turns out most of the simulations range with a fairly small value between 0 to 0.25, while a few cases show a really high deviation. Combined with the comparison between figure 9 and figure 10, we think our simulated aftershocks provide a relatively accurate result in Los Angeles earthquakes map.

Although we find a small value of spatial magnitude deviation, there are issues with this method. First, we ignore the time component, which can result in an inaccurate calculation. For example, a simulated aftershock happened three years later than the actual earthquakes. In this case, we can't really relate them together because of this long time gap. Since we find aftershocks normally don't last longer than a few years, there is little correlation between them, and therefore we shouldn't consider that simulated aftershock as a real earthquake. Moreover, when using this method, only $\frac{1}{4}$ of simulated earthquakes were found to match with real earthquakes, but others are all discarded. Since we only include locations of simulated earthquake that exactly match with historical data,

some earthquakes that have a close location are discarded, and therefore this method of quantification needs great improvement.

From our model, we find great potential of reproducing historical aftershocks with simulated earthquakes. To better apply them, we may use these simulated data to predict future earthquakes. In the future, ETAS simulation can be generated millions of times and then they can be applied with the transformer model,[2] to provide more accurate earthquake results, and help people to accurately predict the aftershocks of earthquakes.

Conclusion

In this paper, we use ChatGPT to help us generate a Python code of ETAS model, and we find it follows the three statistical laws. As a beginner in earthquake research, Artificial Intelligence, ChatGPT, does provide a good access to learn and study the ETAS model. It can provide the python code of the ETAS model with detailed instructions and descriptions of each part, which is more convenient and better than the R code provided from previous research.[20] Also, ChatGPT greatly saves the time of writing the code on my own since I don't have enough experience to code in geophysical area, and it may take me several months to make the code that ChatGPT can reach within a few seconds. Since this code provides great accuracy, it is always better to take advantage of this efficiency. Then we apply this AI-generated ETAS model in the Los Angeles area to simulate the aftershocks from 1969 to 2024. Compared with real earthquake data, simulations show some similar patterns such as the some large magnitude earthquakes, as well as the trend of small earthquakes, but it also shows some unexpected earthquakes and ignores some strong aftershocks. Lastly, we develop a method to quantify this inaccuracy by calculating its spatial magnitude deviation ΔM_s and find a fairly small value to show that the deviation between magnitudes is small for earthquakes that happened historically. However, some drawbacks are also discussed for this method. Researchers have been applying this model with a nowcasting technique using Machine Learning recently, and it shows a positive result.[21,22] Therefore, by extensively applying machine learning techniques, we think this model can combine with the transformer model[2] to better predict the aftershocks for future earthquake events.

References

(1) Ogata, Y. Statistical Models for Earthquake Occurrences and Residual Analysis for Point Processes. *Journal of the American Statistical Association* **1988**, *83*, 9–27.

(2) Vaswani, A.; Shazeer, N.; Parmar, N.; Uszkoreit, J.; Jones, L.; Gomez, A. N.; Kaiser, L. u.; Polosukhin, I. Attention is All you Need. Advances in Neural Information Processing Systems. 2017.

(3) Gupta, H. K.; Rekapalli, R. A Short Note on the Aftershock Duration of Strong to Major Himalayan Earthquakes. *Journal of the Geological Society of India* **2022**, *98*, 611–614.

(4) Fan, X.; Juang, C. H.; Wasowski, J.; Huang, R.; Xu, Q.; Scaringi, G.; van Westen, C. J.; Havenith, H.-B. What we have learned from the 2008 Wenchuan Earthquake and its aftermath: A decade of research and challenges. *Engineering Geology* **2018**, *241*, 25–32.

(5) Yong, C.; Booth, D. C. *The Wenchuan Earthquake of 2008: Anatomy of a Disaster*; Springer Berlin Heidelberg: Berlin, Heidelberg, 2011; pp 1–69.

(6) Riga, G.; Balocchi, P. Aftershocks Identification and Classification. *Open Journal of Earthquake Research* **2017**, *2017*, 135–157.

(7) Geist, E. L. In *Advances in Geophysics*; Dmowska, R., Ed.; Advances in Geophysics; Elsevier, 2012; Vol. 53; pp 35–92.

(8) Gutenberg, B.; Richter, C. F. Frequency of earthquakes in California*. *Bulletin of the Seismological Society of America* **1944**, *34*, 185–188.

(9) Felzer, K. Calculating the Gutenberg-Richter b value. *AGU Fall Meeting Abstracts* **2006**, *-1*, 08.

(10) Godano, C.; Lippiello, E.; de Arcangelis, L. Variability of the b value in the Gutenberg-Richter distribution. *Geophysical Journal International* **2014**, *199*, 1765–1771.

(11) Utsu, T. A statistical study on the

occurrence of aftershocks. *Geophysical magazine* **1961**, *30*, 521–605.

(12) Utsu, T.; Ogata, Y.; S, R.; Matsu'ura The Centenary of the Omori Formula for a Decay Law of Aftershock Activity. *Journal of Physics of the Earth* **1995**, *43*, 1–33.

(13) Båth, M. Lateral inhomogeneities of the upper mantle. *Tectonophysics* **1965**, *2*, 483–514.

(14) Schoenberg, F. P. Facilitated Estimation of ETAS. *Bulletin of the Seismological Society of America* **2013**, *103*, 601–605.

(15) Lombardi, A. M. Estimation of the parameters of ETAS models by Simulated Annealing. *Scientific Reports* **2015**, *5*, 8417.

(16) Hainzl, S. ETAS-Approach Accounting for Short-Term Incompleteness of Earthquake Catalogs. *Bulletin of the Seismological Society of America* **2021**, *112*, 494–507.

(17) Hainzl, S.; Christophersen, A.; Rhoades, D.; Harte, D. Statistical estimation of the duration of aftershock sequences. *Geophysical Journal International* **2016**, *205*, 1180–1189.

(18) Helmstetter, A.; Kagan, Y. Y.; Jackson, D. D. Comparison of Short-Term and Time-Independent Earthquake Forecast Models for Southern California. *Bulletin of the Seismological Society of America* **2006**, *96*, 90–106.

(19) Kattamanchi, S.; Tiwari, R. K.; Ramesh, D. S. Non-stationary ETAS to model earthquake occurrences affected by episodic aseismic transients. *Earth, Planets and Space* **2017**, *69*, 157.

(20) Davoudi, N.; Tavakoli, H. R.; Zare, M.; Jalilian, A. Aftershock probabilistic seismic hazard analysis for Bushehr province in Iran using ETAS model. *Natural Hazards* **2020**, *100*, 1159–1170.

(21) Rundle, J. B.; Yazbeck, J.; Donnellan, A.; Fox, G.; Ludwig, L. G.; Heflin, M.; Crutchfield, J. Optimizing Earthquake Nowcasting With Ma-

chine Learning: The Role of Strain Hardening in the Earthquake Cycle. *Earth and Space Science* **2022**, *9*, e2022EA002343, e2022EA002343 2022EA002343.

(22) Rundle, J. B.; Baughman, I.; Zhang, T. Nowcasting Earthquakes With Stochastic Simulations: Information Entropy of Earthquake Catalogs. *Earth and Space Science* **2024**, *11*, e2023EA003367, e2023EA003367 2023EA003367.

Appendix

Our ETAS code is very long and complicated so it is posted on `https://github.com/JameZ233/ETAS_CODE_TZ.git`. In this paper, Artificial Intelligence (ChatGPT) is only used during the python code developing. In particular, it helps to write the function generate_catalog in ETASCalcV5.py, which initially runs the simulation.